

Human-Guided Planner for Non-Prehensile Manipulation

Rafael Papallas and Mehmet R. Dogar

Abstract—We present a human-guided planner for non-prehensile manipulation in clutter. Most recent approaches to manipulation in clutter employs randomized planning, however, the problem remains a challenging one where the planning times are still in the order of tens of seconds or minutes, and the success rates are low for difficult instances of the problem. We build on these control-based randomized planning approaches, but we investigate using them in conjunction with human-operator input. We show that with a minimal amount of human input, the low-level planner can solve the problem faster and with higher success rates.

I. INTRODUCTION

We present a human-guided planner for non-prehensile manipulation in clutter. We show example problems in Figs. 1 and 2. The target of the robot is to reach and grasp the green object. To do this, however, the robot first has to push other objects out of the way (Fig. 1b to Fig. 1e). This requires the robot to plan which objects to contact, where and how to push those objects so that it can reach the goal object.

These *reaching through clutter* problems are difficult to solve due to several reasons: First, the number of objects make the state space of high-dimensionality. Second, this is an underactuated problem, since the objects cannot be controlled by the robot directly. Third, predicting the evolution of the system state requires running computationally expensive physics simulators, to predict how objects would move as a result of the robot pushing. Effective algorithms have been developed [1]–[11], however the problem remains a challenging one, where the planning times are still in the order of tens of seconds or minutes, and the success rates are low for difficult problems.

Further study of the reaching through clutter problem is important to develop approaches to solve the problem more successfully and faster. It is a problem that has a potential for major near-term impact in warehouse robotics and personal home robots. The algorithms that we currently have, however, are not able to solve reaching through clutter problems in the real world in a fast and consistent way. Here, we ask the question of whether human-operators can be used to provide a minimal amount of input that results in a significantly higher success rate and faster planning times.

Most recent approaches to the reaching through clutter problem employs the power of randomized *kinodynamic*

This research has received funding from the European Union’s Horizon 2020 research and innovation programme under the Marie Skłodowska-Curie grants agreement No. 746143, and from the UK Engineering and Physical Sciences Research Council under grant EP/N509681/1, EP/P019560/1 and EP/R031193/1.

Authors are with the School of Computing, University of Leeds, United Kingdom {r.papallas, m.r.dogar}@leeds.ac.uk

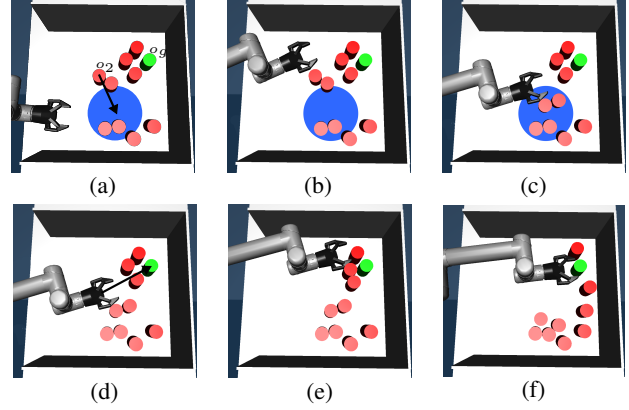


Fig. 1: A human-operator guiding a robot to reach for the green goal object, o_g . Arrows indicate human interaction with the robot. In (a) the operator indicates o_2 to be pushed to the blue target region. From (a) to (c) the robot plans to perform this push. In (d) the operator indicates to the robot to reach for the goal object. From (d) to (f) the robot plans to reach the goal object.

planning. Haustein et al. [4] use a kinodynamic RRT [12], [13] planner to sample and generate a sequence of robot pushes on objects to reach a goal state. Muhayyuddin et al. [5] use the KPIECE algorithm [14] to solve this problem. These planners report some of the best performance (in terms of planning times and success rates) in this domain so far.

We build on these kinodynamic planning approaches, but we investigate using them in conjunction with human-operator input. In our framework, the human operator supplies a *high-level plan* to make the underlying planners solve the problem faster and with higher success rates.

II. PROBLEM FORMULATION

Our environment is comprised of a robot r , a set of movable obstacles O , and other static obstacles. The robot is allowed to interact with the movable obstacles, but not with the static ones. We also have $o_g \in O$ which is the *goal* object to reach.

We are interested in problems where the robot needs to reach for an object in a cluttered shelf that is constrained from the top, and therefore we constrain the robot motion

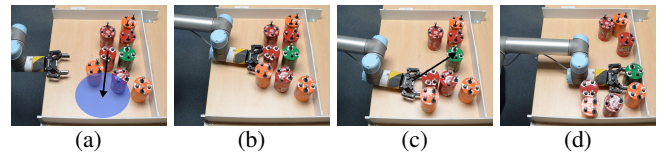


Fig. 2: Human-operator guiding a robot in the real-world.

to the plane and its configuration space, Q^r , to $SE(2)$. The configuration of a movable object $i \in \{1, \dots, |O|\}$, q^i , is its pose on the plane (x, y, θ) . We denote its configuration space as Q^i . The configuration space of the complete system is the Cartesian product $Q = Q^r \times Q^g \times Q^1 \times \dots \times Q^{|O|-1}$.

Let $q_0 \in Q$ be the initial configuration of the system, and $Q_{goals} \subset Q$ a set of possible goal configurations. A goal configuration, $q_n \in Q_{goals}$, is defined as a configuration where o_g is within the robot's end-effector (see Fig. 1f).

Let U be the control space comprised of the robot velocities. Let the system dynamics be defined as $f : Q \times U \rightarrow Q$ that propagates the system from $q_t \in Q$ with a control $u_t \in U$.

We define the *Reaching Through Clutter* (RTC) problem as the tuple $(Q, U, q_0, Q_{goals}, f)$. The solution to the problem is a sequence of controls from U that move the robot from q_0 to a $q_n \in Q_{goals}$.

III. SAMPLING-BASED KINODYNAMIC PLANNERS

Two well known sampling-based kinodynamic planners are Rapidly-exploring Random Trees (RRT) [12], [13] and Kinodynamic Motion Planning by Interior-Exterior Cell Exploration (KPIECE) [14]. We use kinodynamic RRT and KPIECE in our work in two different ways: (1) as baseline RTC planners to compare against, and (2) as the low-level planners for the Guided-RTC Framework that accepts high-level actions (explained in Sec. IV).

In this work, when we plan with a kinodynamic planner (either RRT or KPIECE) we will use the notation *kinodynamicPlanning*(q_{start} , $goal$) with a start configuration of the system, q_{start} , and some *goal* input.

IV. GUIDED-RTC FRAMEWORK

In this section we describe a *guided* system to solve RTC problems. A Guided-RTC system accepts high-level actions. A high-level action can suggest to push a particular obstacle object into a certain region, or it may suggest to reach for the goal object. We formally define a high-level action with the triple (o_i, x_i, y_i) , where $o_i \in O$ is an object, and (x_i, y_i) is the centroid of a *target region* that o_i needs to be pushed into. The target region has a constant diameter d .

In this work, we investigate how a Guided-RTC system with a human-in-the-loop performs when compared with (a) solving the original RTC problem directly using kinodynamic approaches (Sec. III), and (b) using Guided-RTC systems with automated ways of generating the high-level actions.

A. A Generic approach for Guided-RTC Planning

We present a generic algorithm for Guided-RTC in Alg. 1. The next high-level action is decided based on the current configuration (line 4). If the object in the high-level action is not the goal object (line 5), then it is pushed to the target region between lines 6 and 11, and a new high-level action is requested. If it is the goal object, the robot tries to reach it between lines 13 and 15 and the system terminates.

We plan to push an object to its target region in two steps. On line 7 we plan to an intermediate *approaching state* near the object, and then on line 9, we plan from this approaching

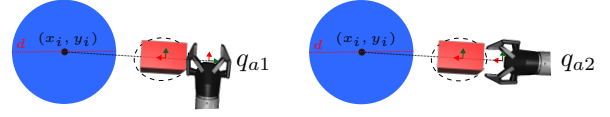


Fig. 3: Approaching states: The blue circle is the target region, the red rectangle the object to manipulate. We compute two approaching states, q_{a1} and q_{a2} .

state to push the object to its target region. Specifically, given an object to push, o_i , we compute two approaching states q_{a1} and q_{a2} (line 6). Fig. 3 shows how these approaching states are computed, based on the object's current position, the centroid (x_i, y_i) and the minimum enclosing circle of the object. The approaching state q_{a1} encourages side-ways pushing, where q_{a2} encourages forward pushing. We also experimented with planning without first approaching the object but we found that approaching the object from a good pose yields to faster pushing solutions. Using both approaching states as the goal we plan to move to one of them (multi-goal planning) on line 7. Then, from the approaching state reached (either q_{a1} or q_{a2}) we push o_i to its target region (line 9). If any of the two planning calls on lines 7 and 9 fails, then the algorithm proceeds to the next high-level action (line 4). Otherwise, we execute the solutions sequentially on line 11, which changes the current system configuration $q_{current}$.

Alg. 1 runs up to an overall time limit, $T_{overall}$, or until a goal is reached. The pushing planning calls on lines 7 and 9 have their own shorter time limit, $T_{pushing}$, and they should find a valid solution within this limit. The planning call on line 13 is allowed to run until the overall time limit is over.

B. Guided-RTC with Human-In-The-Loop (GRTC-HITL)

Guided-RTC with Human-In-The-Loop (GRTC-HITL) is an instantiation of the GRTC Framework. A human-operator, through a graphical user interface, provides the high-level actions. In Alg. 2 we present GRTC-HITL NEXTHIGHLEVELACTION function (referenced in Alg. 1, line 4).

The human provides high-level actions until she selects

Algorithm 1 Guided-RTC

```

1: procedure GRTC( $Q, U, q_0, Q_{goals}$ )
2:    $q_{current} \leftarrow q_0$ 
3:   do
4:      $o_i, x_i, y_i \leftarrow \text{NEXTHIGHLEVELACTION}(q_{current})$ 
5:     if  $o_i \neq o_g$  then
6:        $q_{a1}, q_{a2} \leftarrow \text{compute approaching states to } o_i$ 
7:        $\text{kinodynamicPlanning}(q_{current}, \{q_{a1}, q_{a2}\})$ 
8:       if planning fails then continue
9:        $\text{kinodynamicPlanning}(q_{a1} \text{ or } q_{a2}, (o_i, x_i, y_i))$ 
10:      if planning fails then continue
11:       $q_{current} \leftarrow \text{execute solutions from lines 7 and 9}$ 
12:    while  $o_i \neq o_g$ 
13:     $\text{kinodynamicPlanning}(q_{current}, Q_{goals})$ 
14:    if planning succeeds then
15:       $q_{current} \leftarrow \text{execute solution from line 13}$ 

```

Algorithm 2 GRTC-HITL

```

1: function NEXTHIGHLEVELACTION( $q_{current}$ )
2:    $o_i \leftarrow$  get object selection from human operator
3:   if  $o_i \neq o_g$  then
4:      $x_i, y_i \leftarrow$  get region centroid from human operator
5:     return  $o_i, x_i, y_i$ 
6:   return  $o_g$ 

```

Algorithm 3 GRTC-Heuristic Planner

```

1: function NEXTHIGHLEVELACTION( $q_{current}$ )
2:    $o_b \leftarrow$  find the first blocking obstacle to  $o_g$ 
3:   if there exists a blocking obstacle  $o_b$  then
4:      $x_b, y_b \leftarrow$  find collision-free placement of  $o_b$ 
5:     return  $o_b, x_b, y_b$ 
6:   return  $o_g$   $\triangleright$  No blocking obstacle, reach the goal

```

the goal object, o_g . The GRTC framework (Alg. 1) plans and executes them. The state of the system changes after each high-level action and the human operator is presented with the resulting state each time ($q_{current}$). Note here that *the operator can decide not to provide any guidance*.

We developed a simple user interface to communicate with the human-operator. The operator, using a mouse pointer, provides the input by first clicking on the desired object and then a point on the plane (Fig. 1a) that becomes the centroid of the target region.

The approach we propose here uses a human-operator to decide on the high-level plan. One question is whether one can use automatic approaches, and how they would perform compared to the human suggested actions. To make such a comparison, we implemented an automated approach (GRTC-Heuristic, Sec. IV-C).

C. Guided-RTC with Straight Line Heuristic (GRTC-Heuristic)

We present this approach in Alg. 3 and illustrate it in Fig. 4. This heuristic assumes the robot moves on a straight line from its current position towards the goal object (Fig. 4b). The first blocking object, o_b on line 2, is identified as the next object to be moved. During the straight line motion, we capture the robot’s swept volume, V_{swept} (Fig. 4b). We randomly

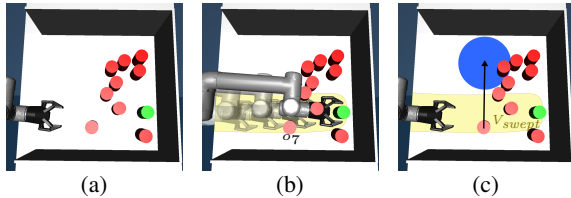


Fig. 4: GRTC-Heuristic: (a) Initial state. (b) The robot moves on a straight line to the goal object, o_g , to obtain the first blocking obstacle (o_b) and the swept volume (yellow area). (c) The heuristic produces a high-level action for o_b indicated by the arrow and the target region (blue). This process is repeated until V_{swept} contains no blocking obstacle.

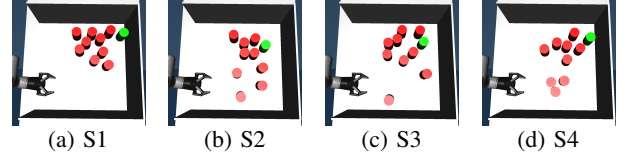


Fig. 5: Initial states of different problems in simulation (S1-S4). Goal object is in green.

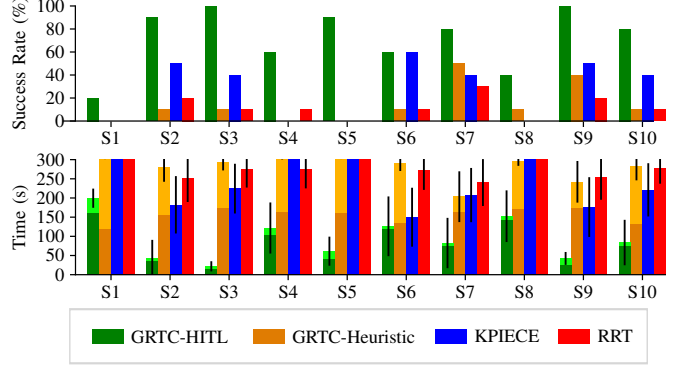


Fig. 6: Simulation results, for each scene (S1-S10): (Top) Success rate. (Bottom) Mean planning time. The error bars indicate the 95% CI. For GRTC-HITL and GRTC-Heuristic, the dark shade indicates the planning time where the light shade indicates the time it took to produce the high-level actions (for GRTC-HITL this is a fraction of the time).

sample a collision-free target region centroid outside V_{swept} (Alg. 3 line 4 and Fig. 4c). The object and the centroid are then returned as the next high-level action (Alg. 3 line 5).

After every high-level action suggested by the heuristic, the Guided-RTC framework (Alg. 1) plans and executes it and the state of the system is updated ($q_{current}$). The heuristic then suggests a new high-level action from $q_{current}$ until there is no blocking obstacle (Alg. 3 line 6).

V. EXPERIMENTS & RESULTS

For all experiments, we use the Open Motion Planning Library (OMPL) [15] implementation of RRT and KPIECE. We use MuJoCo¹ [16] to implement the system dynamics, f . For all planners, the overall planning time limit, $T_{overall}$, is 300 seconds, after which it was considered a failure. For GRTC-HITL and GRTC-Heuristic, $T_{pushing}$ is 10 seconds.

A. Simulation Results

We evaluated each approach 100 times by running them 10 times in 10 different, randomly-generated, scenes. Some of the scenes are presented in Figs. 5a to 5d. For GRTC-HITL, the human-operator interacted with each scene *once* and from the last state left by the human-operator we ran the planner (Alg. 1 line 13) to reach for the goal object *10 times*.

Fig. 6 summarizes the results of our experiments for each of the random scenes (S1-S10). Fig. 6-Top shows that GRTC-HITL yields to more successes per scene than any other approach except for S6 which was as successful as KPIECE.

¹On a computer with Intel Core i7-4790 CPU @ 3.60GHz, 16GB RAM.

The overall success rate for each approach is 72% for GRTC-HITL, 11% for RRT, 28% for KPIECE and 14% for GRTC-Heuristic. Fig. 6-Bottom shows that GRTC-HITL improved the planning time in *all* scenes.

Table I summarizes the guidance performance for GRTC-HITL and GRTC-Heuristic for all ten scenes. Proposed Actions indicates the total number of high-level actions proposed. This number includes the successful actions (actions that the planner managed to satisfy) and failed actions (actions that the planner could not find a solution for). Guidance Time indicates the time spent on generating the high-level actions in seconds (in case of GRTC-HITL the time the human-operator was interacting with the system and for GRTC-Heuristic the time took for the heuristic to generate the high-level actions).

B. Real-robot results

We performed experiments using a UR5 manipulator on a Ridgeback omnidirectional base. We used the OptiTrack motion capture system to detect initial object/robot poses and to update the state in the human interface after every high-level action.

We evaluated RRT, KPIECE and GRTC-HITL performance in *ten* different problems in the real world.

Table II summarizes the success rate of each approach in the real world. When we say that the robot failed during execution, we mean that although the planner found a solution, when the robot executed the solution in the real-world, it either failed to reach the goal object, or it violated some constraint (hit the shelf or dropped an object to the floor). These execution failures were due to the uncertainty in the real world: The result of the robot's actions in the real-world yield to different states than the ones predicted by the planner.

The success rate for GRTC-HITL, RRT and KPIECE is 70%, 20%, and 10% respectively. GRTC-HITL failed 20% during planning and 10% during execution. KPIECE was more successful during planning than RRT but failed most of the times during execution. RRT, on the other, hand accounts for more failures during planning than any other approach.

In Fig. 2 we show an example. The human operator provides the first high-level action in Fig. 2a and then indicates the goal object in Fig. 2c which is reached in Fig. 2d.

VI. CONCLUSIONS

We introduced a new human-in-the-loop framework for physics-based non-prehensile manipulation in clutter (GRTC-

HITL). We showed through simulation and real-world experiments that GRTC-HITL is more successful and faster in finding solutions than the three baselines we compared with.

REFERENCES

- [1] M. Dogar, K. Hsiao, M. Ciocarlie, and S. Srinivasa, "Physics-based grasp planning through clutter," in *Robotics: Science and Systems*, 2012.
- [2] G. Havur, G. Ozbilgin, E. Erdem, and V. Patoglu, "Geometric rearrangement of multiple movable objects on cluttered surfaces: A hybrid reasoning approach," in *Robotics and Automation (ICRA), 2014 IEEE International Conference on*. IEEE, 2014, pp. 445–452.
- [3] N. Kitaev, I. Mordatch, S. Patil, and P. Abbeel, "Physics-based trajectory optimization for grasping in cluttered environments," in *2015 IEEE International Conference on Robotics and Automation (ICRA)*. IEEE, 2015, pp. 3102–3109.
- [4] J. A. Haustein, J. King, S. S. Srinivasa, and T. Asfour, "Kinodynamic rearrangement planning via dynamic transitions between statically stable states," in *Robotics and Automation (ICRA), 2015 IEEE International Conference on*. IEEE, 2015, pp. 3075–3082.
- [5] M. ud din, M. Moll, L. Kavraki, J. Rosell *et al.*, "Randomized physics-based motion planning for grasping in cluttered and uncertain environments," *IEEE Robotics and Automation Letters*, vol. 3, no. 2, pp. 712–719, 2018.
- [6] W. Bejjani, R. Papallas, M. Leonetti, and M. R. Dogar, "Planning with a receding horizon for manipulation in clutter using a learned value function," in *2018 IEEE-RAS 18th International Conference on Humanoid Robots (Humanoids)*. IEEE, 2018, pp. 1–9.
- [7] W. Bejjani, M. R. Dogar, and M. Leonetti, "Learning physics-based grasping in clutter: Combining image-based generalization and look-ahead planning," in *2019 IEEE/RSJ International Conference on Intelligent Robots and Systems (IROS)*. IEEE, 2019.
- [8] J. E. King, M. Cognetti, and S. S. Srinivasa, "Rearrangement planning using object-centric and robot-centric action spaces," in *2016 IEEE International Conference on Robotics and Automation (ICRA)*. IEEE, 2016, pp. 3940–3947.
- [9] W. C. Agboh and M. R. Dogar, "Real-time online re-planning for grasping under clutter and uncertainty," in *2018 IEEE-RAS 18th International Conference on Humanoid Robots (Humanoids)*. IEEE, 2018, pp. 1–8.
- [10] E. Huang, Z. Jia, and M. T. Mason, "Large-scale multi-object rearrangement," in *2019 International Conference on Robotics and Automation (ICRA)*. IEEE, 2019, pp. 211–218.
- [11] K. Kim, J. Lee, C. Kim, and C. Nam, "Retrieving objects from clutter using a mobile robotic manipulator," in *2019 16th International Conference on Ubiquitous Robots (UR)*. IEEE, 2019, pp. 44–48.
- [12] S. M. LaValle, "Rapidly-exploring random trees: A new tool for path planning," 1998.
- [13] S. M. LaValle and J. J. Kuffner Jr, "Randomized kinodynamic planning," *The international journal of robotics research*, vol. 20, no. 5, pp. 378–400, 2001.
- [14] I. A. Şucan and L. E. Kavraki, "Kinodynamic motion planning by interior-exterior cell exploration," in *Algorithmic Foundation of Robotics VIII*. Springer, 2009, pp. 449–464.
- [15] I. A. Şucan, M. Moll, and L. E. Kavraki, "The Open Motion Planning Library," *IEEE Robotics & Automation Magazine*, vol. 19, no. 4, pp. 72–82, December 2012, <http://ompl.kavrakilab.org>.
- [16] E. Todorov, T. Erez, and Y. Tassa, "Mujoco: A physics engine for model-based control," in *Intelligent Robots and Systems (IROS), 2012 IEEE/RSJ International Conference on*. IEEE, 2012, pp. 5026–5033.

TABLE I: Simulation results.

	GRTC-HITL		GRTC-Heuristic	
	μ	σ	μ	σ
Proposed Actions	4.9	3.3	88.4	58.2
Successful Actions	3.1	1.0	3.0	1.4
Guidance Time (s)	13.6	10.0	124.3	81.7

TABLE II: Real-world results.

	GRTC-HITL	KPIECE	RRT
Successes	7	1	2
Planning Failures	2	4	8
Execution Failures	1	5	0